523

NPS-PH-91-002PR

NAVAL POSTGRADUATE SCHOOL
Monterey, California

ANNUAL SUMMARY OF BASIC RESEARCH IN
. THERMOACOUSTIC HEAT TRANSPORT: 1990

ANTHONY A. ATCHLEY

THOMAS J. HOFLER

OCTOBER 1990

Annual Report

Approved for Public Release; distribution unlimited

Prepared for:

f Naval Research
Division Code 1112
n, VA 22217-5000

Reproduction of all or part of this report is authorized.

This report was prepared by:

REPORT DOCUMENTATION PAGE

1a REPORT SECURITY CLASSIFICATION	1b RESTRICTIVE MARKINGS
UNCLASSIFIED	

2a SECURITY CLASSIFICATION AUTHORITY	3 DISTRIBUTION / AVAILABILITY OF REPORT
2b DECLASSIFICATION / DOWNGRADING SCHEDULE	Approved for public release; distribution unlimited

4 PERFORMING ORGANIZATION REPORT NUMBER(S)	5 MONITORING ORGANIZATION REPORT NUMBER(S)
NPS-PH-91-002PR	

6a NAME OF PERFORMING ORGANIZATION	6b OFFICE SYMBOL (If applicable)	7a NAME OF MONITORING ORGANIZATION
Naval Postgraduate School	PH	Office of Naval Research

6c ADDRESS (City, State, and ZIP Code)	7b ADDRESS (City, State, and ZIP Code)
Physics Department Naval Postgraduate School Monterey, CA 93943-5000	Physics Division, Code 1112 Arlington, VA 22217-5000

8a NAME OF FUNDING SPONSORING ORGANIZATION	8b OFFICE SYMBOL (If applicable)	9. PROCUREMENT INSTRUMENT IDENTIFICATION NUMBER
ONR		N00014-90-WR-24001

8c ADDRESS (City, State, and ZIP Code)	10 SOURCE OF FUNDING NUMBERS			
	PROGRAM ELEMENT NO	PROJECT NO	TASK NO	WORK UNIT ACCESSION NO
Arlington, VA	61153N		4126949	

11 TITLE (Include Security Classification)

ANNUAL SUMMARY OF BASIC RESEARCH IN THERMOACOUSTIC HEAT TRANSPORT: 1990

12 PERSONAL AUTHOR(S)

Atchley, A. A. (Physics Department Code PH/Ay) & Hofler, T. J. (Physics Dept. Code PH/Hf)

13a TYPE OF REPORT	13b TIME COVERED	14 DATE OF REPORT (Year, Month, Day)	15 PAGE COUNT
Annual summary	FROM 01Oct89 TO 30Sep90	901031	30

16 SUPPLEMENTARY NOTATION

17 COSATI CODES			18 SUBJECT TERMS (Continue on reverse if necessary and identify by block number)
FIELD	GROUP	SUB-GROUP	Thermoacoustic heat transport; prime mover; heat pump; heat engine
20	01		
20	13		

19 ABSTRACT (Continue on reverse if necessary and identify by block number)

This annual report details progress in basic research in thermoacoustic heat transport made during the period October 1, 1989 through September 30, 1990. Four projects are discussed. The first project involves measurements of thermoacoustic phenomena using thermoacoustic couples (TACs). The purpose of the second project is to examine means of visualizing thermoacoustic processes. The third project is an investigation of heat driven prime movers. The fourth project considers the performance of thermoacoustic heat engines that operate with an acoustic sound field that is not a perfect standing wave. A publications, patents, presentations, and honors report is also included.

20 DISTRIBUTION / AVAILABILITY OF ABSTRACT	21 ABSTRACT SECURITY CLASSIFICATION
☒ UNCLASSIFIED UNLIMITED ☐ SAME AS RPT ☐ DTIC USERS	UNCLASSIFIED

22a NAME OF RESPONSIBLE INDIVIDUAL	22b TELEPHONE (Include Area Code)	22c OFFICE SYMBOL
L. E. Hargrove	(202) 696-4221	ONR Code 1112

DD FORM 1473, 84 MAR   83 APR edition may be used until exhausted   SECURITY CLASSIFICATION OF THIS PAGE
All other editions are obsolete

☆ U.S. Government Printing Office 1986—606-24.

UNCLASSIFIED

ABSTRACT

This annual report details progress in basic research in thermoacoustic heat transport made during the period October 1, 1989 through September 30, 1990. Four projects are discussed. The first project involves measurements of thermoacoustic phenomena using thermoacoustic couples (TACs). The purpose of the second project is to examine means of visualizing thermoacoustic processes. The third project is an investigation of heat driven prime movers. The fourth project considers the performance of thermoacoustic heat engines that operate with an acoustic sound field that is not a perfect standing wave. A publications, patents, presentations, and honors report is also included.

A. INTRODUCTION

The purpose of this research project is to investigate thermoacoustic heat transport phenomena. The premise of the majority of this research can be summarized as follows. While early measurements of thermoacoustic phenomena qualitatively agree quite well with the theory developed by Wheatley[1] and Swift,[2] there have been few thorough, quantitative comparisons of measurement and theory. The quantitative studies that have been performed previous to our involvement indicate that the theory does not adequately explain the results.[3]

Thermoacoustic phenomena and the associated devices can be described in terms of two basic modes of operation, heat pumps and prime movers. In thermoacoustic heat pumps, an acoustic field stimulates the transport of entropy over the surface of an object, resulting in a thermal gradient being established across that object. In prime movers, a thermal gradient is established across an object which is part of, or housed in, an acoustic resonator. At sufficiently high gradients, sound is spontaneously generated in the resonator. The stored thermal energy is converted into acoustic energy; the work output of the device is equal to the energy in the acoustic field. Our study of thermoacoustic processes involves investigating both of these fundamental classes of phenomena. Our previous research has indicated that when the acoustic amplitude is low, measurements and theory agree reasonably well. However, when the amplitude is large, there is considerable disagreement.[4-8] In other words, in the linear acoustic regime, thermoacoustics seems to be relatively well understood, whereas in the nonlinear regime, it is not. The question now arises "Is it the thermoacoustics which in not well understood, or the nonlinear acoustics?"

In FY 1990, we extended our previous measurements and began to investigate ways to separate apparent inadequacies of the theory of thermoacoustics from phenomena caused by nonlinear acoustic affects. In addition, we have begun to consider the performance of thermoacoustic heat engines that operate with an acoustic sound field that is not a perfect standing wave. Pertinent previous results of our investigations, along with a brief discussion of the

progress made during FY 90, follow.

B. SUMMARY OF PROGRAM

Our research program consists of four projects. The first project involves measurements of thermoacoustic phenomena using thermoacoustic couples (TACs). The purpose of the second project is to examine means of visualizing thermoacoustic processes. The third project is an investigation of heat driven prime movers. The fourth project considers the performance of thermoacoustic heat engines that operate with an acoustic sound field that is not a perfect standing wave. Summaries of progress made in these projects during FY 1990 follow.

1. TAC Measurements

We have devoted a large effort to a thorough investigation of basic thermoacoustic phenomena using the simplest class of thermoacoustic engine - a thermoacoustic couple, or TAC. A typical TAC is composed of a stack of short, poorly thermally conducting plates, spaced by at least a few thermal penetration depths. The advantage of using a TAC is that its design allows assumptions to be made which reduce the theory of thermoacoustic heat transport to its simplest form. Our previous research[4-8] has shown that the basic theory agrees relatively well with the result of measurements made at low acoustic intensities. However, there is serious disagreement between theory and experiment at higher acoustic intensities. A major effort prior to FY 90 has been to develop a computer controlled apparatus which would facilitate data acquisition. An extensive set of measurements has been made with this apparatus, which allows us to vary the acoustic pressure amplitude, the position of the TAC, the acoustic frequency, and the mean gas pressure and temperature. These measurements represent one of the most complete studies of thermoacoustic phenomena to date.

3

The first part of FY 90 was devoted to analyzing and communicating the results of the initial, exploratory, phase of the TAC measurements.[9] Several conclusion may be drawn from this work. The first conclusion is that the thermoacoustic effect is relatively, yet not completely, well understood at low values of the drive ratio (the ratio of the peak acoustic pressure amplitude at a pressure antinode to the mean pressure of the gas) for the plate configurations used in these measurements. The second conclusion is that there are two distinct regions of behavior at higher drive ratios. One region, which occurs for drive ratios less that approximately 1.1%, is characterized by a linear decrease in the agreement between theory and experiment. (See Reference 9 for the meaning of "linear decrease in the agreement.") The second region, which occurs for drive ratios greater than approximately 1.1%, is characterized by the onset of irregularities in the temperature difference data series. Also, the linear dependence of the disagreement disappears. Further, because the agreement is, generally, best in the vicinity of the pressure antinode (velocity node), some velocity dependent effect may be the cause of the poor agreement at higher drive ratios, where the acoustic particle displacement amplitude can be as much as a few millimeters. There is also evidence of an effect which depends on the produce of acoustic pressure and velocity.

In light of these results, we have initiated the second phase of the TAC measurements, intended to further probe the discrepancies and behaviors uncovered during the first phase. The first series of measurements is designed to investigate whether or not edge effects become important at the higher drive ratios and are the cause of the irregularities discussed above. In the previous measurements, we measured the temperature difference developed across the TAC with a series of thermocouples (called a thermopile) placed along the front and back edges of the TAC, as illustrated in Fig. 1. Because of its proximity to the edge, the thermopile may be sensitive to effects which, though perhaps causing *local* deviations in the temperature profile, do not affect the temperature profile in interior regions of the plate. In other words, although we observe considerable deviations between theory and measurements made at the plate edges, the interior (and majority) of the plate may behave in accordance with predictions.

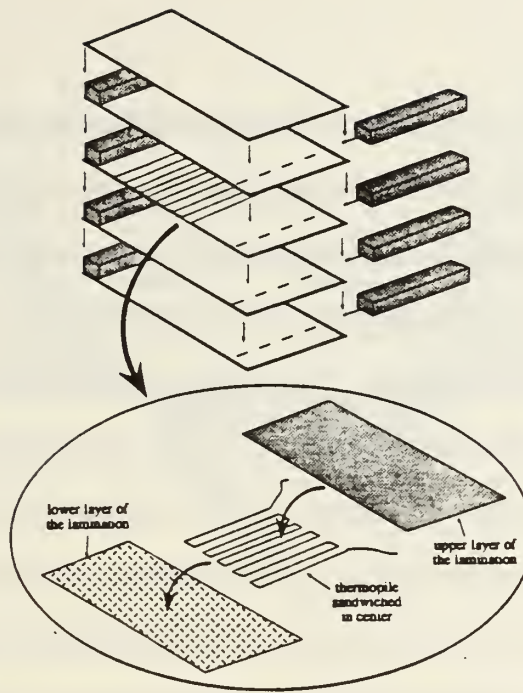It is useful to examine some data taken with a TAC having an edge-to-edge thermopile. An

Figure 1: The general design of a thermoacoustic couple (TAC) used in the measurements. The central plate is instrumented with a thermopile used to measure the temperature difference developed across the TAC. Four guard plates surround the central plate.
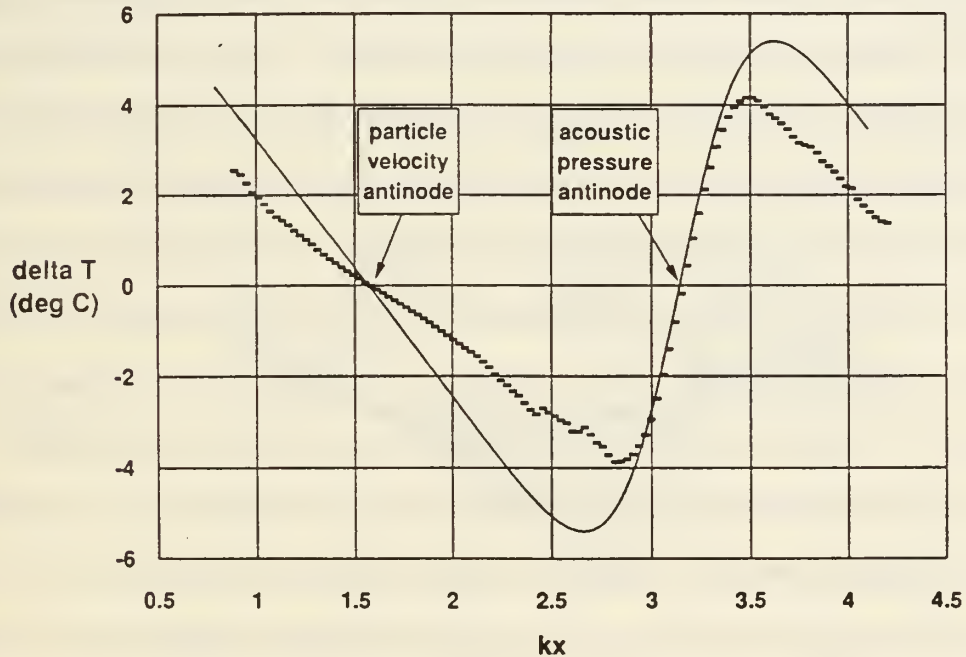

Figure 2: Graph showing the measured (dashed curve) and the theoretical value (solid curve) of the temperature difference developed across a TAC as functions of kx for helium and a drive ratio of 1.99%. The mean gas pressure is 114.1 kPa. The acoustic pressure amplitude is 2.27 kPa and the frequency is 696 Hz. The theoretical temperature difference is computed using Eq. (1) of Ref. 9.

example is shown in Fig. 2, which illustrates the comparison between the measured temperature difference across a TAC (dashed curve) and the theoretical value (solid curve). (Refer to Ref. 9 for full details of the TAC construction and experimental parameters.) The TAC is in helium at 298.4 K. The mean gas pressure and temperature are 114.1 kPa and the acoustic pressure amplitude is 2.27 kPa, giving a drive ratio of 1.99%. The frequency is 696 Hz. The theoretical temperature difference is computed using Eq. (1) of Ref. 9. The temperature differences are plotted as functions of kx, where k is the wave number and x is the location of the center of the TAC. The positions of the particle velocity and pressure antinodes are indicated on the graph. Four areas for comparisons are obvious. First, the agreement is quite good in the vicinity of the pressure antinode. The slopes of the measured and predicted temperature differences are approximately equal. Secondly, the agreement in the vicinity of the velocity antinode is poor. The magnitude of the slope of the measured temperature difference is much less than that of the predicted result. Third, the data series of the measured temperature difference is quite irregular and jagged in the vicinity of the maximum theoretical temperature difference. Finally, the measured maximum temperature difference is less than and occurs at a different position than the predicted maximum. In short, the agreement between theory and experiment is poor except near the pressure antinode.

Figure 3 illustrates the theoretical temperature difference as a function of kx for drive ratios from 0.17 to 1.99% in helium at a mean pressure of 113.8 ± 0.2 kPa, temperature 298.4 ± 0.1 K, and frequency 702.8 ± 4.5 Hz. (The individual values of the drive ratio, mean pressure, temperature and frequency have been omitted, in order to reduce clutter on the graph. The values given above represent the average and standard deviation for the entire data set. The data presented in Fig. 2 is a subset of these data.) This graph clearly indicates the progression from a sinusoid to a sawtooth curve and the displacement of the maximum temperature difference toward the pressure antinode as described by Wheatley et al.[1] The measured temperature differences are shown in Fig. 4 for the same experimental conditions. The measurements do confirm qualitatively the sinusoid-to-sawtooth progression. One of the curves is dashed to demarcate two regions of behavior. The curves between the kx axis and the dashed curve, corresponding to lower drive ratios, are smooth
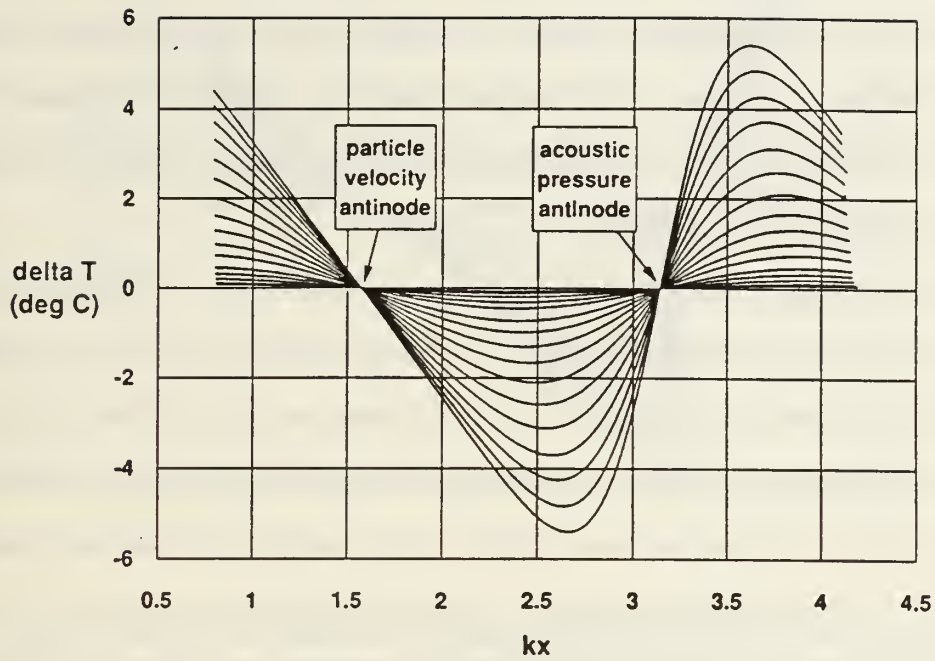
Figure 3: Graph showing the theoretical temperature difference as a function of kx for drive ratios from 0.17 to 1.99% for a TAC in helium at approximately the same mean pressure and frequencies as those in Fig.2. The data presented in Fig. 2 is a subset of these data.

Figure 4: Graph showing the measured temperature difference as a function of kx for drive ratios from 0.17 to 1.99% for a TAC in helium at approximately the same mean pressure and frequencies as those in Fig.2. The data presented in Fig. 2 is a subset of these data.
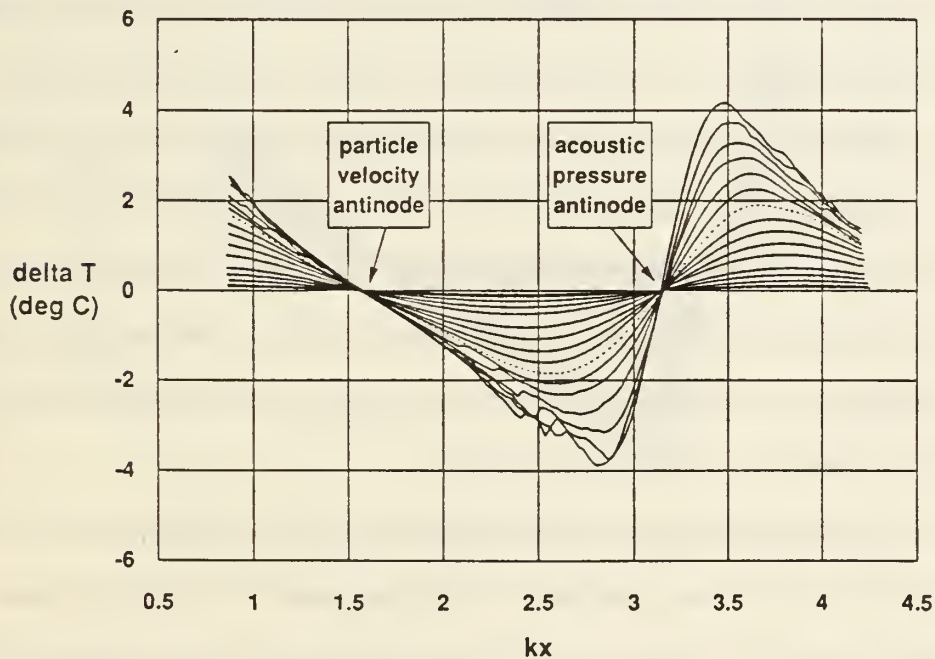
and regular. The curves on the other side of the dashed curve, corresponding to higher drive ratios, become jagged and irregular. This sudden transition occurs in all of the data sets we have taken with TACs having a single thermopile spanning the TAC edge-to-edge. The dashed curve corresponds to a drive ratio of 1.03%.

In order to investigate whether edge effects are the cause of any of these discrepancies, we have constructed a TAC with two thermopiles, whose junctions do not lie along the edge, and repeated some of the previous measurements. Preliminary results are shown in Figs. 5 and 6, which show the temperature difference measured by the two thermopiles as a function of kx. The TAC is 1.495 cm long. The two thermopiles are 1.373 cm and 0.682 cm long and centered on the TAC. Therefore, the thermocouple junctions lie approximately 0.061 cm and 0.407 cm from the edges, respectively. Figure 5 shows the data from the longer thermopile, Fig. 6 from the shorter. The TAC is in helium at a mean gas pressure and temperature of 200 ± 1 kPa and 295.9 ± 0.1 K. The frequency range for the data is 662.8 ± 4.5 Hz. The drive ratio range is 0.20% - 2.70%. The dashed curve in both figures corresponds to a drive ratio 0.97%. (Recall that the dashed curve in Fig. 4 corresponds to a drive ratio of 1.03%.) Comparing these results with those shown in Fig. 4, they are strikingly similar. (No direct comparison is possible since the experimental conditions are different.) Moreover, the transition to an irregular behavior starts at a 1% drive ratio, as it did with the edge-to-edge design. These data show that the temperature profile of the interior of the TAC behaves the same as that measured at the edge. Therefore, the irregularities previously observed are not an artifact of placing the thermopile along the edge. The irregularities may still be the result of the edge (e.g., turbulence generated at the edge), but they are not isolated at the edge. They extend at least half way to the center of the TAC.

We will continue this series of measurements in FY 1991 to further identify the extent of these irregularities and determine their cause. We also intend to extend our measurements to geometries other than TACs, in order to see to what extent the observed behavior is present in more useful thermoacoustic engine stacks.
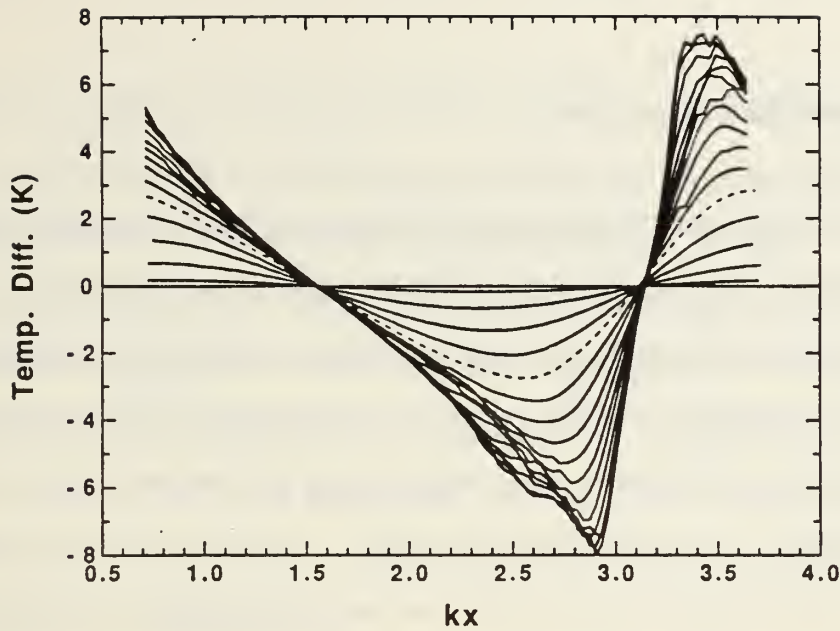
Figure 5: Graph showing the temperature difference developed across a TAC as measured with the longer of the two thermopiles. The TAC is in helium at a mean gas pressure and temperature of 200 ± 1 kPa and 295.9 ± 0.1 K. The frequency range for the data is 662.8 ± 4.5 Hz. The drive ratio range is 0.20% - 2.70%. The dashed curve in both figures corresponds to a drive ratio 0.97%.
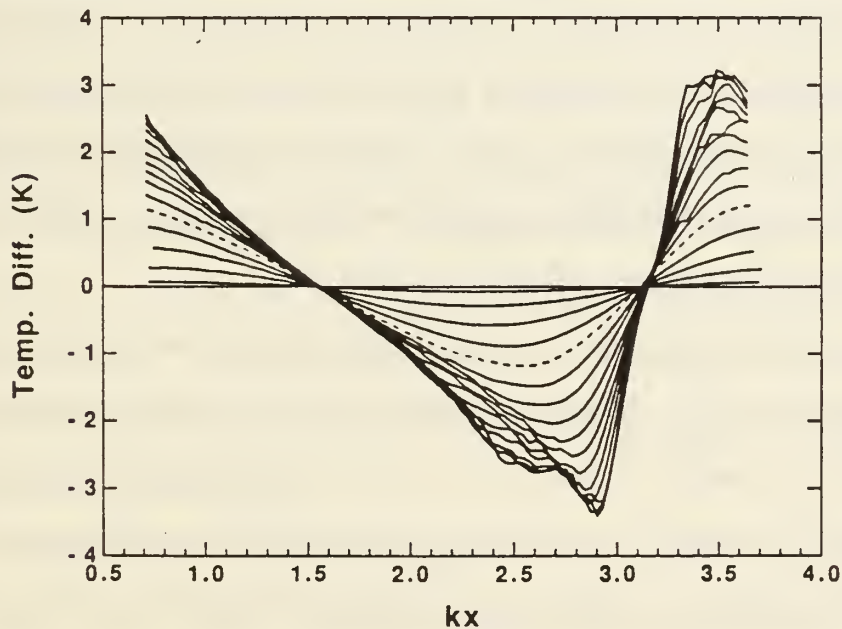

Figure 6: Graph showing the temperature difference developed across a TAC as measured with the shorter of the two thermopiles. The experimental conditions are the same as those in Fig. 5. The dashed curve in both figures corresponds to a drive ratio 0.97%.

2. Visualization of Thermoacoustics

It is assumed in the theory applied to our TAC measurements that all parts of the plate behave in the same manner, that edge effects and other complicating factors do not exist. Therefore, if such factors do occur it is important to know about them. One way to investigate whether or not these complications play any significant role in our experiments is to make measurements such as those described above. However, these measurements with thermopiles give only the average temperature difference across portions of the plate. They do not give the actual temperature distribution. Perhaps a better way is to find a method to "visualize" the temperature distribution. This notion involves a completely different measurement technique.

Two methods of visualizing thermoacoustics are apparent. One technique, proposed by us previously, is to utilize a thermal imaging camera in order to photograph, in the infrared, a plate or stack of plates exposed to an acoustic standing wave. The result would be a real time image of the evolution of the temperature gradients in the plate and could yield information about thermoacoustic heat transport which can not be gained using discrete thermocouples. A thermal imaging camera is available in the Electro-Optics laboratory in the NPS Physics Department. However, there are several disadvantages associated with its use. Because the resolution of these disadvantages could prove expensive, we have decided to initially investigate a second, though less sophisticated, technique to determine whether visualization is fruitful at all.

In this second technique, strips of liquid crystal, temperature sensitive, sheets replace, for instance, the plates of a TAC. When these strips are exposed to a large amplitude acoustic standing wave, a visible color gradient is setup in the strip. We have constructed a transparent, Plexiglas resonator in which to conduct the experiment so that the strips are readily visible. The strips have a 5 °C temperature range over which the color changes from brown to green as the temperature increases. When a standing wave is setup, the color change occurs quickly. Within a few seconds, the edge of the strip closest the nearest pressure antinode turns green, while the other edge turns brown. As time progresses, the green and brown regions expand toward the center of

the strip, forming a uniform temperature gradient across the strip. Eventually, the mean temperature of the strip rises and the overall color pattern shifts towards green. Finally, the entire strip indicates that the temperatures are out of the temperature range of the strip.

Several important results arise from these preliminary experiments. The extreme edges change color first, demonstrating that the transported heat accumulates at the edges of the plates first, as first pointed out by Wheatley et al.[1] A uniform gradient is established only after thermal conduction acts to destroy this initial temperature gradient. These observations are entirely consistent with the present understanding of thermoacoustics. A final, yet not unexpected, result is that mean temperature of the plate increases.

Although, we have made only preliminary investigations with the liquid crystal method of visualizing thermoacoustics, the method has already yielded useful qualitative information. Aside from these benefits, this technique is very useful for demonstrating thermoacoustics.[10]

3. Heat Driven Prime Movers

The largest effort in FY 90 has been devoted to the investigation of heat driven prime movers. There are two distinct regions of operation of a prime mover - below and above the onset of self-oscillation. We are investigating each. In an effort to establish a thermoacoustics research program at the University of Mississippi, Professor Henry Bass spent his Sabbatical leave at NPS to learn from our experience. He has been actively involved in the prime mover research. This exchange has not been unidirectional. Dr. Bass's expertise in propagation of sound in porous media has been invaluable to our efforts.

In order to investigate the work output of a prime mover below onset, use is made of the fact that the conversion of thermal energy to acoustic energy affects the net absorption of acoustic energy in the prime mover. As the temperature difference across the prime mover stack (See Fig. 7.) increases from zero to its value at onset, the net absorption decreases to zero. The absorption coefficient can be determined by measuring the quality factor Q of the prime mover, which in turn,
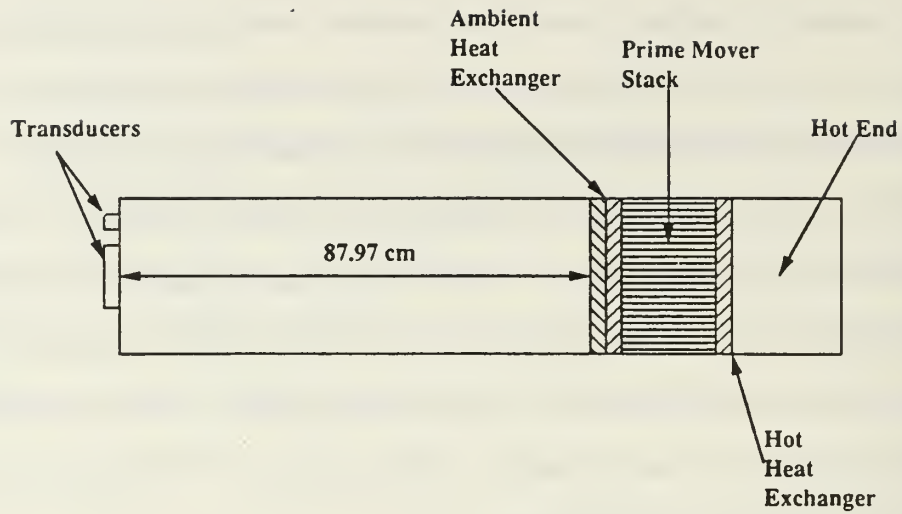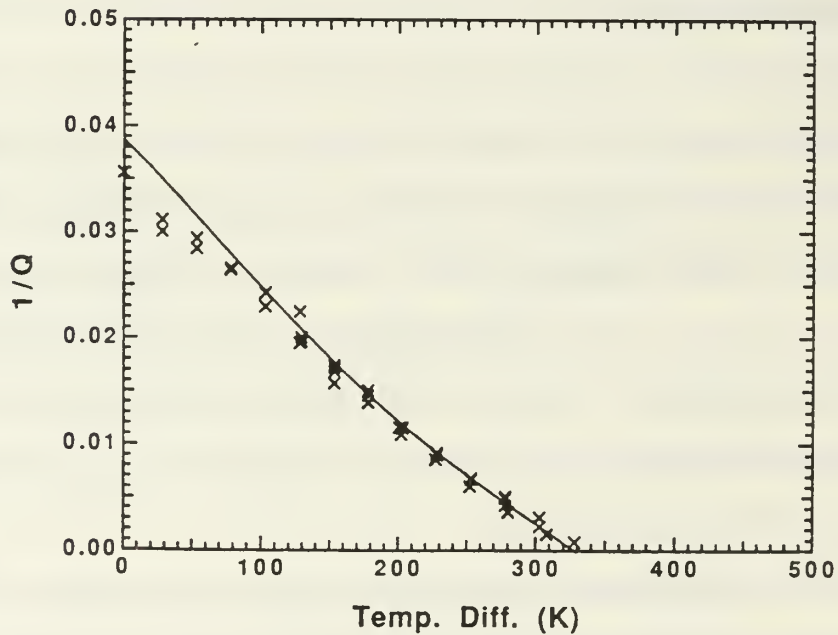
Figure 7:   Diagram of a thermoacoustic prime mover.

Figure 8:   Graph of 1/Q vs the temperature difference across the prime mover stack filled with helium at a mean pressure of 238 kPa. The curve is the results of calculations discussed in Ref. 11.

can be related to the acoustic power dissipated in the tube. The dissipated power can be calculated using equations derived by Swift,[2] which express the acoustic power output of a thermoacoustic engine as a function of the applied temperature difference across the stack. The absorption coefficient can also be extracted from the propagation constant, as is commonly done in porous media calculations.[11]

An example of data taken below the onset of self-oscillation is shown in Fig. 8, which is a graph of 1/Q, proportional to the net absorption coefficient, as a function of the temperature difference across the prime mover stack.[12] The data were obtained by driving the prime mover in the vicinity of its fundamental resonance and measuring the frequency response. It is important to point out that the acoustic levels involved are well within the linear regime. The curve is based on calculations discussed in Ref. 11. Though the overall agreement is quite good, there are some discrepancies. There is a tendance to over predict the absorption at low temperature differences. Although not so obvious from Fig. 8, other data sets indicate some difficulty in predicting the onset temperature The exact reasons for these discrepancies are not entirely clear. What is clear is that certain aspects of the theory have not been adequately addressed.

We have also studied prime movers above the onset of self-oscillation.[13] The prime mover is said to have reached "onset" when the temperature difference across the stack is sufficient for the prime mover to generate and sustain detectable levels of sound. The use of the word "detectable" is not meant to imply that onset is a subtle question of detection thresholds. When onset is reached, the observer (and everyone else in the room) knows it.

Once onset of self-oscillation is reached, the acoustic amplitude in the tube immediately assumes a large value, typically about 1% of the ambient pressure. The observed waveform is noticeably non-sinusoidal. As more energy is supplied to the hot end of the stack, the temperature of that end increases only slightly while the acoustic amplitude in the tube increases rapidly, reaching as much as 7% of ambient pressure. Unfortunately, as the acoustic amplitude increases, an increasing fraction of the acoustic energy appears as higher harmonics - harmonic distortion increases. It is this distortion that has occupied our interest. In order to understand this

phenomena, we must not only fully understand harmonic generation from finite amplitude standing waves but also any contributing nonlinear generation from the thermoacoustics.

Figures 9 and 10 show the waveform and the spectrum of the sound generated by the prime mover above onset. The gas is helium at a mean pressure of 307 kPa. The temperature difference across the stack is 325 °C, which is slightly above onset. The signal exhibits slight distortion, particularly in the positive cycle. Figure 10 shows that the difference in spectrum level between the first few modes is larger than 15 dB. Figures 11 and 12 show results for a temperature difference of 368 °C, the signal is distorted sharply in both positive and negative half-cycles. The difference between spectrum levels for the first few modes has decreased further to less than 6 dB and more energy has been spread to higher modes.

There can be little doubt that the signals at the higher frequencies are being generated by the fundamental. If we examine the frequency of these spectral peaks, they are integral multiples of the fundamental to within four significant digits and have no measurable line width. Prediction of harmonic generation (one method of describing the non-sinusoidal waveform) is not straight forward even with a good understanding of dissipation mechanisms in the stack. In a resonant tube, the frequencies of the overtones depend upon dispersion while harmonic generation results in exact multiples of the fundamental. This means that sound generated nonlinearly will be generated at a frequencies different from tube resonances.

We have applied a treatment of finite amplitude standing waves by Coppens and Sanders[14] which allows us to calculate the the strengths of the harmonics relative to that of the fundamental. Performing the calculations for the situation represented in Figs. 9 and 10 yields (P_2/P_1) = -20 dB and (P_3/P_1) = -32 dB. Referring to Fig. 10 shows that the measured values are closer to -16 and -32 dB, respectively, in reasonable agreement with theory. For the case shown in Fig. 12 the calculations predict (P_2/P_1) = -7 dB and (P_3/P_1) = -8 dB while the measured values are -7.6 and -14.5 dB, respectively. At even higher fundamental amplitudes, the results are less acceptable. Although the results of this analysis are not extremely accurate, they do serve as a motivation to carry the treatment further. The reasons for the discrepancies are not clear.
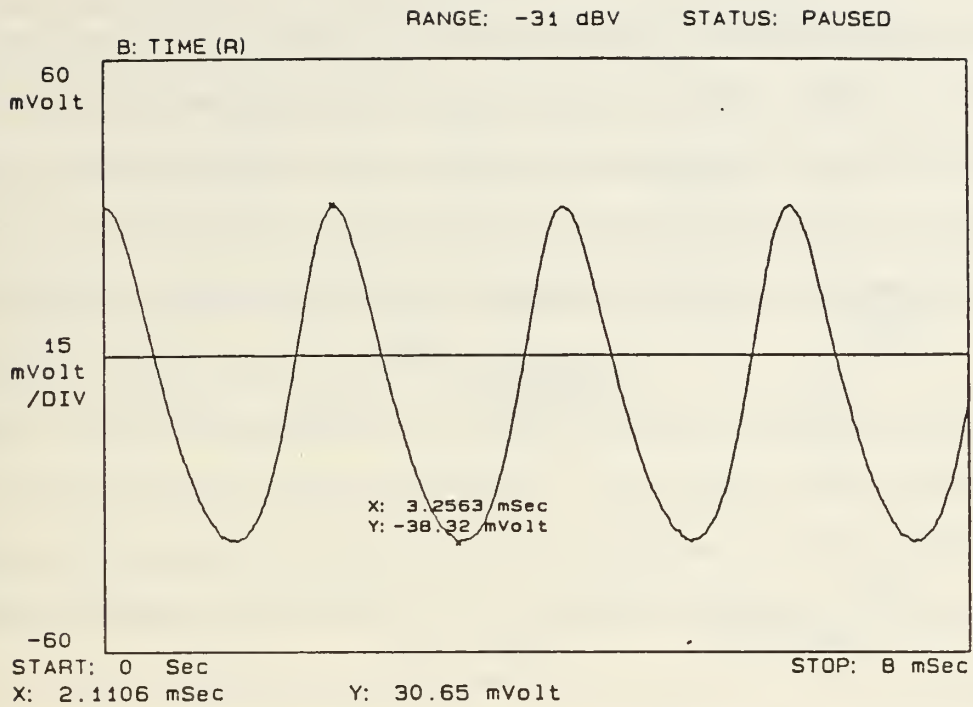
Figure 9: Waveform of the sound generated by the prime mover at a temperature difference of 325°C.
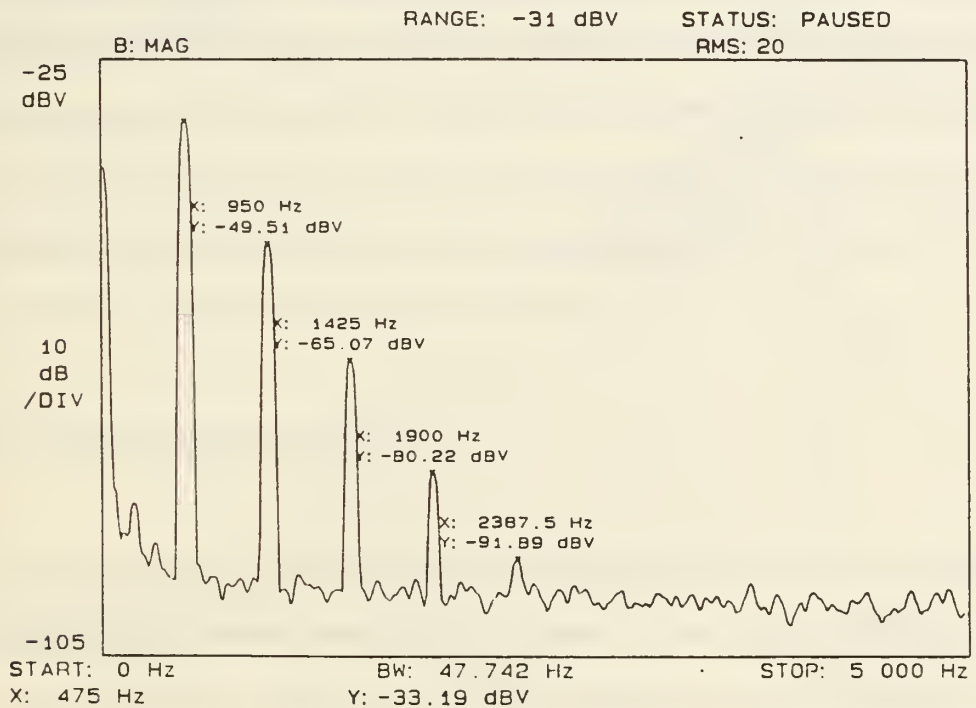
Figure 10: Spectrum of the waveform shown in Fig. 9.

15

RANGE: -19 dBV   STATUS: PAUSED

A: TIME (R)

```
200
mVolt



50
mVolt
/DIV
                    X:  2.6332 mSec
                    Y: -76.31 mVolt



-200
```
START: 0   Sec   STOP: 8 mSec
X: 1.2261 mSec   Y: 126.1 mVolt
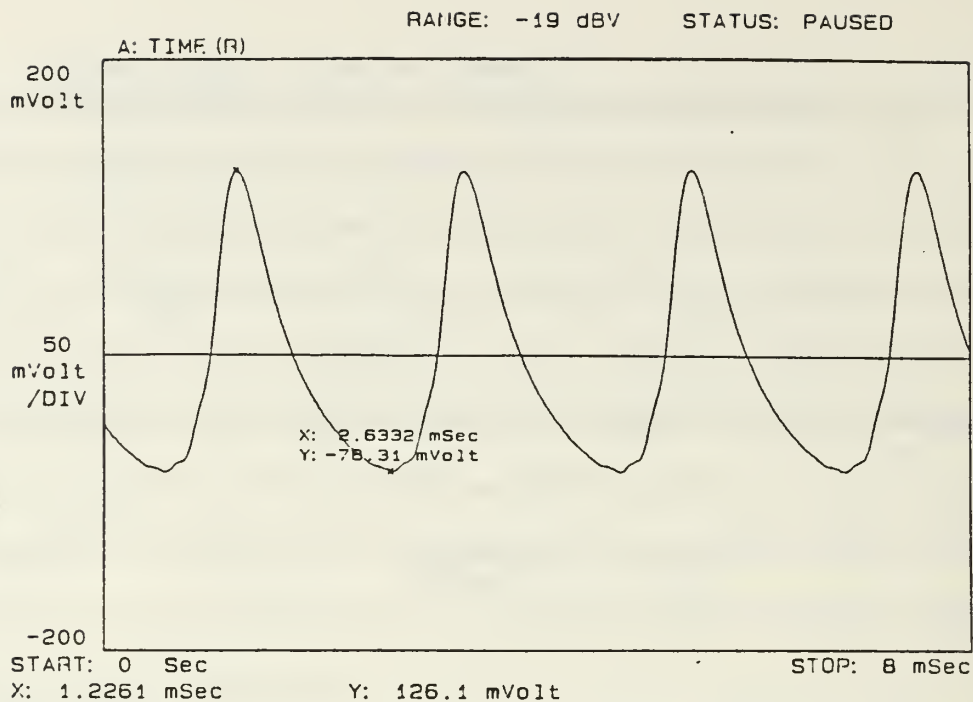
Figure 11: Waveform of the sound generated by the prime mover at a temperature difference of 368°C.

RANGE: -19 dBV   STATUS: PAUSED
                                             RMS: 20

A: MAG

```
-20
dBV
     X:  950 Hz
     Y: -32.29 dBV

         X:  1450 Hz
         Y: -39.84 dBV

            X:  1925 Hz
            Y: -46.79 dBV
               X:  2400 Hz
               Y: -52.57 dBV



10
dB
/DIV




-100
```
START: 0 Hz   BW: 95.485 Hz   STOP: 10 000 Hz
X: 475 Hz   Y: -24.28 dBV

Figure 12: Spectrum of the waveform shown in Fig. 11.

16

At this point, we are not in a position to determine the relative contributions from nonlinear propagation and thermoacoustic generation to the observed waveform distortion. At the very minimum, such a determination will require an accurate model for dispersion in the prime mover. This area is receiving attention now. Beyond that, the equations which give rise to acoustic gain have been linearized. A numerical solution of the coupled momentum and energy equation might identify significant nonlinear terms in the coefficient of gain.
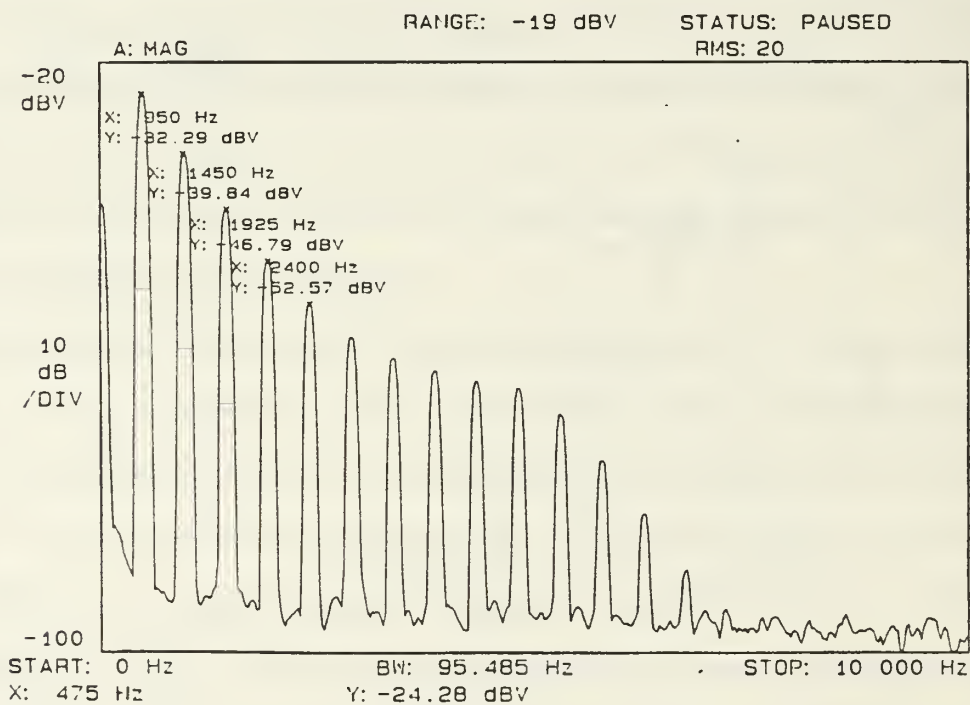
One aspect of prime movers that has been ignored until now is their ability to go into self-oscillation for more than one mode simultaneously. In our prime mover, the temperature difference required for onset for the fundamental mode is approximately 320 °C, while that for the first overtone (the second mode) is 465 °C. By introducing a disk with a hole of the right dimensions in it into the resonator at the right place, we are able increase the onset temperature difference for the fundamental without affecting that for the second mode. This allows us to excite both modes simultaneously. If the attenuator (disk) is not used for the fundamental, we are unable to supply enough power to the prime mover to reach onset for the second mode. The fundamental transports too much heat! As one might imagine, the spectrum of the waveforms generated is quite rich, containing harmonics of both modes as well as sum and difference frequencies. One reason for exciting both modes is that it gives a measure of the dispersion in the prime mover, a quantity needed to understand the harmonic generation discussed above. It also provides another test bed for theory. We intend to pursue these measurements further.

4. Non-perfect Standing Wave Heat Engines

It is of interest to consider the performance of thermoacoustic heat engines that operate with an acoustic sound field that is not a perfect standing wave. In such a system the phase between acoustic pressure and acoustic velocity is somewhere between zero and 90 degrees. This is a difficult theoretical problem to consider in any generality, given the complexity of the problem. The complexity can be seen in the large parameter space required to describe any specific engine.

There are gas parameters: sound speed, Prandtl number, c_p/c_v, and mean pressure. There are stack geometry parameters: plate separation, plate thickness, and stack length. There are operating conditions: acoustic pressure amplitude, velocity amplitude, their relative phase, frequency, and the heat load on a heat pumping stack or the work load on a prime mover stack. These parameters could be expressed differently and equivalently.

The differential equations of N. Rott[15,16] are capable of describing the system with all the detail that we need. The only significant limitation of these equations is that they are linear and are expected to compare well with experimental results only at low acoustic amplitudes. In some ways, these equations require that too many parameters and initial conditions be specified. Some of the parameters can be eliminated by realizing that not all of them are independent, and that the parameter space can be reduced to a minimal independent set by using fairly obvious normalizations. Two examples are: expressing the distances in the wave propagation direction in terms of wavelength units, and expressing distances in the orthogonal diffusion direction in terms of penetration depth units. However, the reduced set of parameters is still complex, and this interferes with the study of generalized questions such as the significance of acoustic phasing.

In an effort to simplify the equations of Rott, Swift[2] makes additional approximations. The first approximation is that the length of the stack is infinitesimally short, and the second is that the spacing between plates in the stack is at least several boundary layers in size, such that the diffusive part of the thermal wave is nearly attenuated to zero at the midpoint between two plates.

The approximation of short stack length is a reasonable way of simplifying the system, at least for our present purposes. For the purpose of analyzing many real or potential experimental systems, the approximation is not very accurate. However, for this study, there is not any substantial loss of information. For example, a finite length stack could be analyzed accurately by modeling it as many infinitesimal stacks placed in series. In fact, this is roughly equivalent to the method used by numerical algorithms for solving ordinary differential equations.

The boundary layer approximation is a severe limitation for this study. The parameter space of interest lies somewhere between two extremes. One extreme is the "classic" thermoacoustic heat

engine as described by Wheatley[1] and Swift[2]. This engine operates in a sound field that has acoustic pressure and acoustic velocity in quadrature, and the spacing between plates of the stack is at least several penetration depths. The other extreme is the Stirling cycle engine, which has the dynamic pressure and velocity in phase, and the spacing between plates of the "regenerator" much less than a penetration depth. Clearly, the boundary layer approximation is not suitable for an analysis of engines that approach the Stirling cycle extreme.

Our approach will be to use Swift's[17] equations initially, and then use the Rott[15,16] equations with the short stack approximation for the actual study of acoustic phasing. Swift's equations for acoustically stimulated enthalpy flow H_2 and acoustic work flow W_2 are,

$$H_2 = \frac{1}{4} \Pi \delta_\kappa \frac{T_m \beta p_1^s \langle u_1^s \rangle}{(1 + \varepsilon_s)(1 + \sigma)(1 - \delta_v/y_o + \delta_v^2/2y_o^2)} \left[\Gamma \frac{1 + \sqrt{\sigma} + \sigma + \sigma\varepsilon_s}{1 + \sqrt{\sigma}} - \left(1 + \sqrt{\sigma} - \frac{\delta_v}{y_o} \right) \right]$$

$$- \Pi (y_o K + l K_s) \frac{dT_m}{dx} ,$$

and

$$W_2 = \frac{1}{4} \Pi \delta_\kappa \Delta x \frac{(\gamma - 1) \omega (p_1^s)^2}{\rho_m a^2 (1 + \varepsilon_s)} \left[\frac{\Gamma}{(1 + \sqrt{\sigma})(1 - \delta_v/y_o + \delta_v^2/2y_o^2)} - 1 \right]$$

$$- \frac{1}{4} \Pi \delta_\kappa \Delta x \frac{\omega \rho_m \langle u_1^s \rangle^2}{1 - \delta_v/y_o + \delta_v^2/2y_o^2} .$$

The initial use of Swift's equations will assist in developing the analysis structure with a simplified set of equations before moving to the more complicated Rott equations. Also the initial analysis can be compared to some of Swift's own results for purposes of error checking, and the final analysis can again be compared to the initial analysis in limiting cases.

Another technique that can be applied to our problem is the graphical display of engine data,

using more than one independent parameter, such as a contour plot of two independent parameters. Figures 13 and 14 are two such contour plots based on the above equations and a purely reactive standing wave sound field. Figure 13 shows contours for a prime mover engine where the solid contours represent efficiency relative to Carnot (perfect) performance and the dashed contours represent dimensionless power density in the form of acoustic work, for a stack having a fixed temperature difference. Figure 14 shows contours for a heat pump where the solid contours represent COP relative to Carnot performance and the dashed contours represent dimensionless power density in the form of heat flow. The parameters chosen for these plots are typical for engines utilizing a 10 bar helium working fluid with modest acoustic amplitudes. The two independent parameters are kx, which is the normalized position of the stack in the standing wave and Γ, which is the normalized temperature gradient in the stack.

A number of interesting observations can be made from the contour plots. Most engine designs would not choose an operating point that coincides with the region of highest power density (since the efficiency is zero there), nor would one choose an operating point that coincides with the region of highest efficiency (since the power density is quite low there). Instead, a more likely choice of operating point is one that lies somewhere on the curve of best compromise between power density and efficiency. This curve (not shown in the figures) is the one that indicates the path in the Γ - kx plane such that a given sacrifice in efficiency, gains the most in power density (or vice-versa).

The work that remains, is to produce similar contours for engine performance that are based on the Rott equations directly, and then vary the acoustic phasing. Also, numerically producing the curve of best compromise on the contour plots would be useful.

Figure 13: Contour plot for a prime mover. The solid contours represent efficiency relative to Carnot (perfect) performance and the dashed contours represent dimensionless power density in the form of acoustic work, for a stack having a fixed temperature difference.
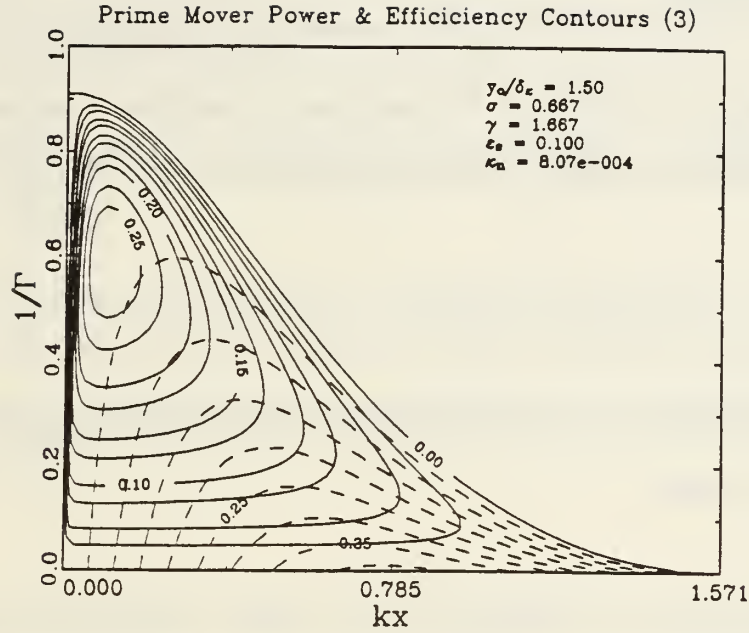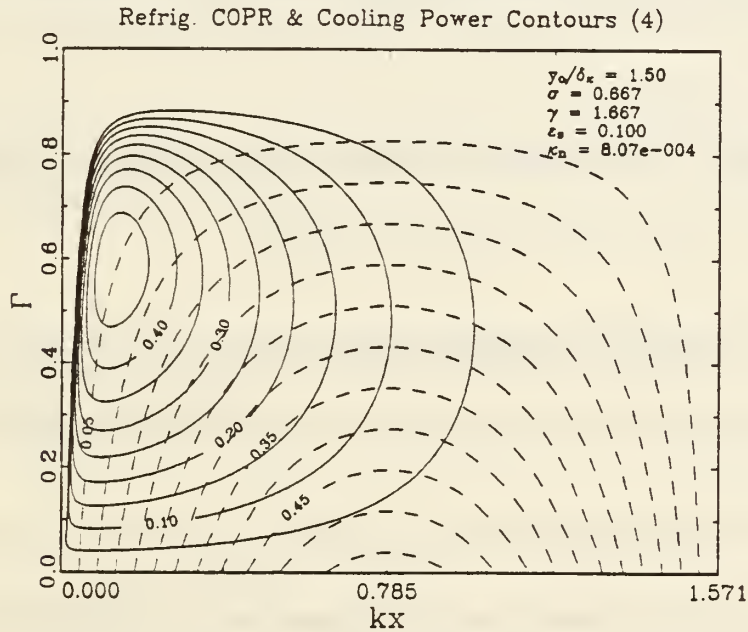

Figure 14: Contour plot for a heat pump. The solid contours represent COP relative to Carnot performance and the dashed contours represent dimensionless power density in the form of heat flow.

C. REFERENCES

1. J. C. Wheatley, T. Hofler, G. W. Swift, and A. Migliori, "An intrinsically irreversible thermoacoustic heat engine," J. Acoust. Soc. Am. 74, 153 - 170(1983).

2. G. W. Swift, "Thermoacoustic engines," J. Acoust. Soc. Am. 84 (4), 1145 - 1180 (1988).

3. A. Migliori and G. W. Swift, "Liquid-sodium thermoacoustic engine," Appl. Phys. Lett. 53 (5), 355-357 (1988).

4. M. L. Muzzerall, A. A. Atchley, and T. J. Hofler, "Acoustically generated temperature gradients in plates", J. Acoust. Soc. Am. 82, Suppl. 1, S21(A) (1987).

5. M. L. Muzzerall, "Investigation of thermoacoustic heat transport using a thermoacoustic couple," Master's Thesis in Engineering Acoustics, Naval Postgraduate School (September 1987).

6. A. A. Atchley, T. J. Hofler and M. D. Kite, "Acoustically generated temperature gradients in short plates," J. Acoust. Soc. Am. 84, S36 (1988).

7. M. D. Kite, "Computerized measurements of thermoacoustically generated temperature gradients," Master's Thesis in Engineering Acoustics, Naval Postgraduate School (December 1988).

8. Ao, Chia-ning, "The Measurement of Thermoacoustic Phenomena Using Thermoacoustic Couples," Master's Thesis in Engineering Acoustics, Naval Postgraduate School (June 1989).

9. A. A. Atchley, T. J. Hofler, M. L. Muzzerall, M. D. Kite, and Chianing Ao, "Acoustically generated temperature gradients in short plates," J. Acoust. Soc. Am. 88 , 251-263 (1990).

10. A. A. Atchley and T. J. Hofler, "Thermoacoustic heat pumps," J. Acoust. Soc. Am. 87, Suppl. 1, S32(A) (1990).

11. Anthony A. Atchley, Henry E. Bass, Thomas J. Hofler, and Hsiao-Tsang Lin, "Study of a thermoacoustic prime mover below onset of self-oscillation," to be submitted for publication in J. Acoust. Soc. Am.

12. Lin, Hsiao-tseng, "Investigation of a heat driven thermoacoustic prime mover," Master's Thesis in Engineering Acoustics, Naval Postgraduate School (December 1989)

13. A. A. Atchley, H. E. Bass and T. J. Hofler, "Development of nonlinear waves in a thermoacoustic prime mover," Frontiers of Nonlinear Acoustics 12th ISNA, edited M. F. Hamilton and D. T. Blackstock (Elsevier Applied Science, New York, 1990), pp. 603-608.

14. A.B. Coppens and J.V. Sanders, "Finite-amplitude standing waves in rigid-walled tubes," J. Acoust. Soc. Am. 43(3), 516-529 (1968).

15 N. Rott, "Damped and thermally driven acoustic oscillations in wide and narrow tubes," Z. Angew. Math. Phys. 20, 230 (1969).

16 N. Rott, "Thermally driven acoustic oscillations, part III: Second order heat flux," Z. Angew. Math. Phys. 26, 43 (1975).

17 Reference 2, Eq. (76) and Eq. (80).

OFFICE OF NAVAL RESEARCH

PUBLICATIONS / PATENTS / PRESENTATIONS / HONORS REPORT

FOR

1 OCTOBER 1989 through 30 SEPTEMBER 1990

****

CONTRACT N00014-90WR24001

R&T NO. 4126949

TITLE OF CONTRACT: BASIC RESEARCH IN THERMOACOUSTIC HEAT TRANSPORT

NAME OF PRINCIPAL INVESTIGATORS: ANTHONY A. ATCHLEY
THOMAS J. HOFLER

NAME OF ORGANIZATION: PHYSICS DEPARTMENT
NAVAL POSTGRADUATE SCHOOL

ADDRESS OF ORGANIZATION: MONTEREY, CA 93943

****

PAPERS SUBMITTED TO REFEREED JOURNALS
(Not yet published.)

N/A

PAPERS PUBLISHED IN REFEREED JOURNALS

Anthony A. Atchley, Thomas J. Hofler, Michael L. Muzzerall, M. David Kite, and Ao, Chia-ning, "Acoustically generated temperature gradients in short plates," J. Acoust. Soc. Am. 88, 251-263, (1990).

PAPERS PUBLISHED IN NON-REFEREED JOURNALS

N/A

TECHNICAL REPORTS PUBLISHED

Anthony A. Atchley, "Annual summary of basic research in thermoacoustic heat transport," Naval Postgraduate School Report Number NPS61-89-015PR, 25 pages, September, 1989.

BOOKS (AND SECTIONS THEREOF) SUBMITTED FOR PUBLICATION

N/A

BOOKS (AND SECTIONS THEREOF) PUBLISHED

A. A. Atchley, H. E. Bass and T. J. Hofler, "Development of nonlinear waves in a thermoacoustic prime mover," Frontiers of Nonlinear Acoustics 12th ISNA, edited M. F. Hamilton and D. T. Blackstock (Elsevier Applied Science, New York, 1990), pp. 603-608.

PATENTS FILED

N/A

PATENTS GRANTED

T. Hofler and S. L. Garrett, "Flexural disk fiber optic interferometric omnidirectional hydrophone," U. S. Patent 4,959,539 granted Sept. 25, 1990.

M. R. Brininstool, J. T. Newmaster, Thomas Hofler, and S. L. Garrett, "Remote fiber optic angular orientation sensor using phase detection of two orthogonal oscillating polarization vectors," U. S. Patent 4,958,072 granted Sept. 18, 1990.

<u>INVITED</u> PRESENTATIONS AT TOPICAL OR SCIENTIFIC/TECHNICAL SOCIETY CONFERENCES

Anthony A. Atchley and Thomas J. Hofler, "Thermoacoustic heat pumps," J. Acoust. Soc. Am. <u>87</u>, Suppl. 1, S32(A) (1990).

Anthony A. Atchley, Steven L. Garrett and Thomas J. Hofler, "Thermoacoustic Heat Transport: Explanations, Demonstrations and Applications," Abstracts of Papers for the 156th National Meeting of the American Association for the Advancement of Science, 45 (1990).

<u>CONTRIBUTED</u> PRESENTATIONS AT TOPICAL OR SCIENTIFIC/TECHNICAL SOCIETY CONFERENCES

A. A. Atchley, H. E. Bass and T. J. Hofler, "Development of nonlinear waves in a thermoacoustic prime mover," <u>Frontiers of Nonlinear Acoustics 12th ISNA</u>, edited M. F. Hamilton and D. T. Blackstock (Elsevier Applied Science, New York, 1990), pp. 603-608.

Anthony A. Atchley, "The past, present and future of cavitation nucleation," presented at the Miniconference on Cavitation and Bubble Dynamics, National Center for Physical Acoustics, Oxford, MS (August 23, 1990).

Anthony A. Atchley, Thomas J. Hofler, and Ao, Chia-ning, "The Measurement of Thermoacoustic

Phenomena Using Thermoacoustic Couples," J. Acoust. Soc. Am. 86, Suppl. 1, S109(A) (1989).

Robert A. Perron and Anthony A. Atchley, "Measurement of Bubble Properties Using a Multi-frequency Sound Field," Meeting of the Canadian Acoustical Society, Halifax, Nova Scotia, Canada, October 1989.

HONORS/AWARDS/PRIZES

Recipient of the Acoustical Society of America's R. Bruce Lindsay award for 1990. (Hofler)

Member of the NPS Physical Acoustics Group which was given the Federal Agency of the Year Award in Science (Given by the Federal Executive Board. 1990 (Atchley & Hofler)

NPS Faculty Performance Award 1990 (Atchley)

GRADUATE STUDENTS SUPPORTED UNDER
CONTRACT FOR YEAR ENDING 30 SEPTEMBER 1989

No support for graduate students is required at the Naval Postgraduate School.

POSTDOCTORALS SUPPORTED UNDER
CONTRACT FOR YEAR ENDING 30 SEPTEMBER 1989

N/A

DISTRIBUTION LIST

Director   1 copy
Defense Advanced Research Projects Agency
Attn: Technical Library, TIO
1400 Wilson Blvd.
Arlington, VA   22209-2309

Office of Naval Research   2 copies
Physics Division Office (Code 1112)
800 North Quincy Street
Arlington, VA   22217-5000

Office of Naval Research   1 copy
Director, Technology (Code 02)
800 North Quincy Street
Arlington, VA   22217-5000

Naval Research Laboratory   1 copy
Department of the Navy (code 2625)
Attn: Technical Library
Washington, DC   20375-5000

Office of the Director of Defense Research and Engineering   1 copy
Information Office Library Branch
The Pentagon, Rm. 3E 1006
Washington, DC   20310

U.S. Army Research Office   2 copies
Box 12211
Research Triangle Park
North Carolina   27709-2211

Defense Technical Information Center   4 copies
Cameron Station
Alexandria, VA   22314

Director   1 copy
National Bureau of Standards
Research Information Center
Attn: Technical Library (Admin E-01)
Gaithersburg, MD   20899

Commander   1 copy
U. S. Army
Belvoir Research, Development, and Engineering Center
Attn: Technical Library (STRBE-BT)
Fort Belvior, VA   22060-5606

ODDR&E Advisory Group on Electron Devices 210 Varick Street, 11th Floor New York, NY 10014-4877	1 copy
Air Force Office of Scientific Research Department of the Air FOrce Bolling AFB, DC 22209	1 copy
Air Force Weapons Laboratory Technical Library Kirkland Air Force Base Albuquerque, NM 87117	1 copy
Lawrence Livermore Laboratory Attn: Dr. W. K. Krupke University of California P. O. Box 808 Livermore, CA 94550	1 copy
Harry Diamond Laboratories Technical Library 2800 Powder Mill Road Adelphi, MD 20783	1 copy
Naval Weapons Center Technical Library (Code 753) China Lake, CA 93555	1 copy
Naval Underwater Systems Center Technical Center New London, CT 06320	1 copy
Commandant of the Marine Corps Scientific Advisor (Code RD-1) Washington, DC 20380	1 copy
Naval Ordnance Station Technical Library Indian Head, MD 20640	1 copy
Naval Postgraduate School Technical Library (Code 0212) Monterey, CA 93943	1 copy
Naval Missile Center Technical Library (Code 5632.2) Point Mugo, CA 93010	2 copies
Naval Ordnance Station Technical Library Louisville, KY 40214	1 copy

Commanding Office   1 copy
Naval Ocean Research & Development Activity
Technical Library
NSTL Station, MS 39529

Naval Oceans Systems Center   1 copy
Technical Library
Silver Spring, MD 20910

Naval Ship Research and Development Center   1 copy
Central Library (Codes L42 and L43)
Bethesda, MD 20084

Naval Avionics Facility   1 copy
Technical Library
Indianapolis, IN 46218

Director   1 copy
Research Administration (Code 81)
Naval Postgraduate School
Monterey, CA 93943

Professor Anthony A. Atchley   5 copies
Physics Department (Code PH/Ay)
Naval Postgraduate School
Monterey, CA 93943

Professor Thomas J. Hofler   1 copy
Physics Department (Code PH/Hf)
Naval Postgraduate School
Monterey, CA 93943